Atmos. Chem. Phys., 13, 9217–9232, 2013
www.atmos-chem-phys.net/13/9217/2013/
doi:10.5194/acp-13-9217-2013

Atmospheric Chemistry and Physics Open Access

Airborne hydrogen cyanide measurements using a chemical ionisation mass spectrometer for the plume identification of biomass burning forest fires

M. Le Breton[1], A. Bacak[1], J. B. A. Muller[1], S. J. O'Shea[1], P. Xiao[2], M. N. R. Ashfold[2], M. C. Cooke[2], R. Batt[2], D. E. Shallcross[2], D. E. Oram[3], G. Forster[4], S. J.-B. Bauguitte[5], and C. J. Percival[1]

[1]The Centre for Atmospheric Science, School of Earth, Atmospheric and Environmental Sciences, University of Manchester, Simon Building, Brunswick Street, Manchester, M13 9PL, UK
[2]School of Chemistry, University of Bristol, Cantock's Close, Bristol, BS8 1TS, UK
[3]National Centre for Atmospheric Science, School of Environmental Sciences, University of East Anglia, Norwich, NR4 7TJ, UK
[4]School of Environmental Sciences, University of East Anglia, Norwich, NR4 7TJ, UK
[5]Facility for Airborne Atmospheric Measurements (FAAM), Building 125, Cranfield University, Cranfield, Bedford, MK43 0AL, UK

Correspondence to: C. J. Percival (carl.percival@manchester.ac.uk)

Received: 31 January 2013 – Published in Atmos. Chem. Phys. Discuss.: 27 February 2013
Revised: 18 July 2013 – Accepted: 19 July 2013 – Published: 16 September 2013

Abstract. A chemical ionisation mass spectrometer (CIMS) was developed for measuring hydrogen cyanide (HCN) from biomass burning events in Canada using I^- reagent ions on board the FAAM BAe-146 research aircraft during the BORTAS campaign in 2011. The ionisation scheme enabled highly sensitive measurements at 1 Hz frequency through biomass burning plumes in the troposphere.

A strong correlation between the HCN, carbon monoxide (CO) and acetonitrile (CH_3CN) was observed, indicating the potential of HCN as a biomass burning (BB) marker. A plume was defined as being 6 standard deviations above background for the flights. This method was compared with a number of alternative plume-defining techniques employing CO and CH_3CN measurements. The 6-sigma technique produced the highest R^2 values for correlations with CO. A normalised excess mixing ratio (NEMR) of 3.68 ± 0.149 pptv ppbv^{-1} was calculated, which is within the range quoted in previous research (Hornbrook et al., 2011). The global tropospheric model STOCHEM-CRI incorporated both the observed ratio and extreme ratios derived from other studies to generate global emission totals of HCN via biomass burning. Using the ratio derived from this work, the emission total for HCN from BB was 0.92 Tg (N) yr^{-1}.

1 Introduction

Biomass burning (BB) is considered to be a major source of trace gases in the atmosphere (Li et al., 2000, 2003, 2009; Shim et al., 2007) and at levels significant enough to perturb regional and global atmospheric chemistry and composition (Levine, 2000). For example, large boreal forest fires in Russia from 2002 to 2003 were responsible for global growth rates of many trace gases including carbon dioxide and methane (Kasischke et al., 2005; Yurganov et al., 2005; Simpson et al., 2006). Fires in boreal regions are estimated to account for 9 % of global fire carbon emissions (Van der Werf et al., 2010), and their occurrences are predicted to increase by 30 % by 2030, with a 74–118 % increase in area burned by 2100 (Flannigan et al., 2005). The area burned in Canada has increased since 1970 as a result of rising surface temperatures (Gillett et al., 2004; Kasischke and Turtesky, 2006) resulting in an expected doubling of CO_2 equivalent greenhouse gas emissions from Canadian fires (Amiro et al., 2009). Long-range transport of the emissions is enabled in the troposphere and lower stratosphere via convection and pyroconvection (Fromm et al., 2000; Jost et al., 2004; Val Martin et al., 2010). This enables fires not only to impact local and regional air quality (Colarco et al., 2004; Morris et

al., 2006), but also to contribute to climate change (Damoah et al., 2004; Vivchar et al., 2010; Tilmes et al., 2011).

BB is considered to be the major source of HCN in the atmosphere (Li et al., 2000, 2003, 2009; Liang et al., 2007; Shim et al., 2007) via the pyrolysis of N-containing species within the fuel (Johnson and Kang, 1971; Glarborg et al., 2003). Cooking fire emissions of HCN have also been observed in Mexico and Africa (Christian et al., 2010), although concentrations fell below Fourier transform IR (FTIR) detection limits. Singh et al. (2003) observed enhancements of HCN in China which correlated with CH_3Cl indicating a source from hard coal burning for cooking. It must also be noted that biofuel is widely used in China (Streets et al., 2003) although data from Africa suggest emissions of nitriles are negligible (Bertschi et al., 2003; Yokelson et al., 2003). HCN is also known to be emitted from motor exhausts, but is thought to be at negligible levels (Li et al., 2003; Lobert et al., 1991).

HCN has previously been observed from field biomass fires (Hurst et al., 1994a, b; Goode et al., 2000a; Yokelson et al., 2007b; Crounse et al., 2009) and using laboratory biomass combustion systems (Lobert et al., 1991; Holzinger et al., 1999; Christian et al., 2004; Becidan et al., 2007). Column measurements of HCN were measured from the International Scientific Station of Jungfraujoch (ISSJ) by solar infrared (IR) spectroscopy in 1998 during an intense period of biomass burning in the tropics (Rinsland et al., 2000). Akagi et al. (2011, 2013) note the HCN emission ratios between similar fires can vary up to 60 % (Yokelson et al., 2009), from undetectable in wood burning to 3 % in peat fires. Singh et al. (2003) observed a HCN contribution from automobiles and from aircraft over the United States, although sources from automobile exhaust and industrial processes are thought to be negligible in comparison with BB (Lobert et al., 1991; Bange and Williams, 2000; Holzinger et al., 2001). A field experiment also indicated no detectable emissions of HCN from domestic biofuels (Bertschi et al., 2003). Thermodynamic calculations carried out by Boldi (1993) predict that an air parcel associated with lightning strikes could have a chemical composition such that the HCN / CO ratio would be around 10^{-4}. Stribling and Miller (1987) showed that simulated lightning in a laboratory could produce HCN on planets such as Jupiter, strengthening the case that lightning-produced HCN has been observed on this planet (e.g. Podolak and Barnum, 1988). There have been examples where HCN has been observed in lightning perturbed air in the Earth's troposphere (Singh et al., 2007; Liang et al., 2007), making lightning a possible additional source of HCN, although how much is still to be determined.

HCN is lost in the troposphere via the reaction with the hydroxyl radical (OH), creating a lifetime of a few years, although the reaction with singlet oxygen (O^1D) is suggested to be important in the lower stratosphere. Uptake into the ocean is currently thought to be the dominant sink with an inferred global HCN biomass burning source of 1.4–2.9 Tg (N) yr^{-1} and an oceanic saturation ratio of 0.83 (Li et al., 2000). This oceanic loss produces a lifetime of 2–5 months (Li et al., 2000, 2003; Singh et al., 2003). Although HCN may play an insignificant role in atmospheric chemistry (Cicerone and Zellner, 1983), it is thought to be an important source of nitrogen in remote oceanic environments (Li et al., 2000). HCN is currently thought to be a useful tracer of BB as a consequence of its limited sources and sufficiently long atmospheric lifetime (Lobert et al., 1990; Holzinger et al., 1999).

Carbon monoxide (CO), acetonitrile (CH_3CN) and HCN are all currently used as a BB tracer, but a standard approach has not been well defined. Thresholds of CO are used, but CO has many other strong sources (e.g. industrial activity). There can be difficulties in filtering out plumes which do not originate from BB. Recent studies implementing these various methods of identifying a BB plume have resulted in an uncertainty in the ratio of HCN to CO due to the variability observed in fires and potential mixing from other sources (Simpson et al., 2011; Vay et al., 2011; Hornbrook et al., 2011; Yokelson et al., 2009 ; Sinha et al., 2003; Andreae and Merlet., 2001). Using measurements of HCN and CO, BB plumes can be uniquely identified; enabling emission factors to be calculated from aircraft measurements.

Previous atmospheric measurements of HCN have been made using IR spectroscopy (Coffey et al., 1981; Zhao et al., 2002; Kleinböhl et al., 2006; Rinsland et al., 2007; Li et al., 2000). In situ measurements were first made in the stratosphere using NI-CIMS (negative ion–chemical ionisation mass spectrometer) (Schneider et al., 1997). Tropospheric measurements were then made by long-path Fourier transform IR (FTIR) spectroscopy within BB plumes (Goode et al., 2000a, b; Yokelson et al., 2007b), with a gas chromatography (GC) system, using a reduction gas detector (RGD) (Singh et al., 2003), by NI-CIMS using CF_3O^- as the reagent ion (Crounse et al., 2006, 2009; Yokelson et al., 2007a), and by PTR-MS (proton transfer–mass spectrometry) (Knighton et al., 2009). Crounse et al. (2006) have shown that CIMS can be used to detect HCN selectively in the lower atmosphere, with a low detection limit and at a high frequency. Hornbrook et al. (2011) recently reported HCN to CO ratios from BB plumes using HCN measurements from a chemical ionisation mass spectrometer.

The overall goal of "quantifying the impact of BOReal forest fires on Tropospheric oxidants using Aircraft and Satellites (BORTAS)" campaign was to investigate the connection between the composition and the distribution of biomass burning outflow, ozone production and loss within the outflow, and the resulting perturbation to oxidant chemistry in the troposphere (Palmer et al., 2013). Airborne measurements were taken on board the BAe-146 large atmospheric research aircraft (ARA) over eastern Canada between 12 July and 3 August 2011. The evolution and composition of these BB plumes were studied using the airborne instruments, ground instruments and satellites. In order to study

Table 1. HCN : CO NEMRs (in pptv ppbv^{-1}) for 5 flights during BORTAS campaign in plumes determined by 6 or 10 sigma above background and R^2 of correlations. NEMR units are ppt ppb^{-1}.

Flight	Background (pptv)	1 sigma (pptv)	6 sigma (pptv)	6 sigma slope	10 sigma slope	6 sigma R^2	10 sigma R^2
B621	70	6	107	4.7 ± 0.14	4.68 ± 0.15	0.83	0.83
B622	46	7	88	0.66 ± 0.048	0.66 ± 0.061	0.46	0.46
B624	17	17	173	2.68 ± 0.09	2.68 ± 0.090	0.82	0.79
B626	10	10	245	2.72 ± 0.28	2.82 ± 0.18	0.81	0.83
B628	8	8	108	3.68 ± 0.15	3.3 ± 0.24	0.69	0.45
Average	–	–		2.89 ± 0.15	2.83 ± 0.15	0.72	0.67
Average without B622	–	–		3.45 ± 0.18	3.37 ± 0.18	0.79	0.73

the characteristics of these plumes, an accurate method of plume identification is required. The rapid time response of CIMS utilising the I^- ionisation scheme (Le Breton et al., 2012) is deployed here for HCN measurements. The main aim of this work is to develop a statistical methodology to define BB plumes using HCN measurements and chemical enhancements within the plume which can then determine their emission factors with respect to CO and volatile organic compounds (VOCs).

2 Experimental

2.1 CIMS

A chemical ionisation mass spectrometer (CIMS) was used for real-time detection of HCN. The CIMS instrument employed here was built by the Georgia Institute of Technology as previously described by Nowak et al. (2007) and has been previously described for formic acid measurements (Le Breton et al., 2012). Subsequently various adjustments have been made to the inlet, and these are described in the following section. The schematic in Fig. 1 shows the set-up used and operating conditions of the CIMS on board the airborne platform FAAM BAe-146 research aircraft.

The inlet consisted of 3/8″ OD diameter PFA tubing of length 580 mm, which was heated to 50 °C to reduce surface losses. An orifice of diameter 0.9 mm was positioned at the front of the inlet to restrict the flow to 5.8 SLM. The pressure in the ionisation region was maintained at 19 Torr (133.322 Pa) throughout the flight by controlling the flow of nitrogen into the ionisation region using a mass flow meter.

2.2 Ionisation scheme

The ion–molecule chemistry using iodide ions (I^-) for trace gas detection has been described by Slusher et al. (2004) and was utilised here to detect HCN. A gas mixture of methyl iodide, CH_3I, and H_2O in N_2 is used to obtain reagent ions I^- and water clusters $I^-\cdot(H_2O)$, of which the latter is important for the ionisation of HCN, forming the adduct observed in the mass spectrum (Fig. 2). HCN was ionised by I^- via an adduct reaction,

$$I^- \cdot (H_2O) + HCN \rightarrow HCN \cdot I^- + H_2O, \quad \text{(R1)}$$

which enabled HCN to be detected selectively at $m/z = 154$.

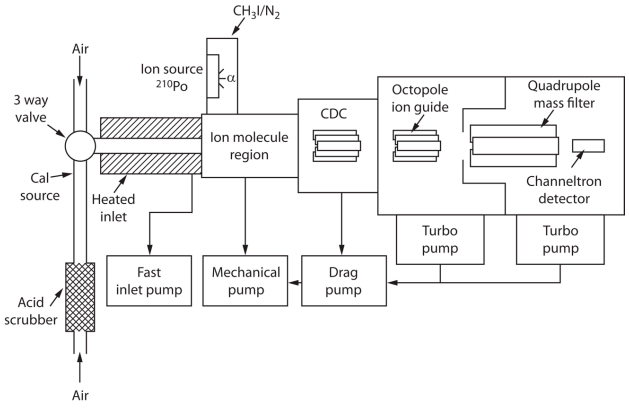

Fig. 1. Schematic of chemical ionisation mass spectrometer (CIMS) used in this study. Arrows indicate direction of gas flow. Dimensions are not to scale.

2.3 HCN calibrations, sensitivity and limit of detection

HCN was calibrated relative to that of formic acid, which was measured and calibrated in-flight throughout the campaign. The sensitivity of HCN relative to formic acid was determined from laboratory calibrations performed with lab air with a relative humidity (RH) ~ 55 % and dry air by passing the lab air through a Drierite dryer. Known concentrations of HCN (Fig. 2) and HCOOH were flowed into the CIMS under these conditions, and sensitivities for both gases were calculated. The BW Technologies HCN calibration cylinder was diluted from a 10 ppm mix with an accuracy of ± 10 %, and the formic acid calibration standard was made as previously described in Le Breton et al. (2012). An average sensitivity ratio of 33 : 1 was observed. The HCN sensitivity was found to be independent of water cluster counts. The ion count signal throughout the flights was normalised to the formic acid

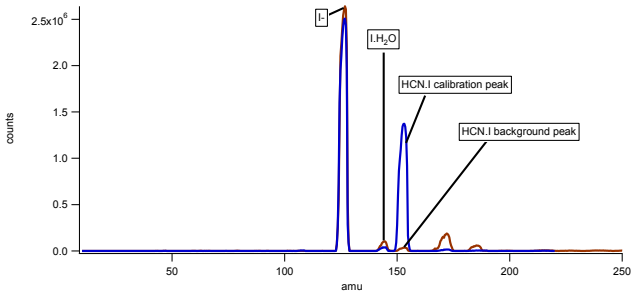

Fig. 2. Mass scan from the CIMS during background (blue line) and encountering a HCN peak at mass 154 (blue line).

sensitivity, which was determined by calibrations before, after and during the flight. The average sensitivity ($\pm 1\sigma$) for each flight was determined by taking the normalised sensitivity and multiplying by the reagent ion count rate to account for reagent ion variability from flight to flight. The average sensitivity for HCN was 4 ± 0.9 Hz pptv^{-1} for 1 MHz of reagent ion signal. The 0.8 Hz data were then averaged over 3 s for the analysis here. The limit of detection for HCN averaged to 3 s was 5 pptv.

2.4 STOCHEM-CRI modelling

The STOCHEM-CRI global chemistry-transport model has been described in detail in several recent papers (Archibald et al., 2010; Cooke et al., 2010a, b, c; Utembe et al., 2009, 2011) and will only be briefly described here. STOCHEM-CRI is a global three-dimensional model, which uses a Lagrangian approach to advect 50 000 air parcels using a fourth-order Runge–Kutta scheme with advection time steps of 3 h (Collins et al., 1997). The transport and radiation models are driven by archived meteorological data, generated by the Met Office numerical weather prediction models as analysis fields with a resolution of 1.25° longitude and 0.83° latitude and on 12 vertical levels extending to 100 hPa (Derwent et al., 2008). The CRI (Common Representative Intermediates) chemical mechanism (CRIv2-R5; Jenkin et al., 2008; Watson et al., 2008; Utembe et al., 2009) has been incorporated into STOCHEM. CRIv2-R5 emits methane and 22 non-methane hydrocarbons. Each air parcel contains the concentrations of 219 species involved in 618 photolytic, gas-phase and heterogeneous chemical reactions, using a 5 min time step. Formation of secondary organic aerosol (SOA) was derived from the oxidation of aromatic hydrocarbons, monoterpenes and isoprene (Utembe et al., 2009, 2011). Surface emissions for CO, NO_x and non-methane hydrocarbons (NMHCs), distributed over five emission types (anthropogenic, biomass burning, vegetation, ocean and soil), are taken from the POET (Precursors of Ozone and their Effects in the Troposphere) inventory (Granier et al., 2012). The distributions for lightning emissions are parameterized based on the work of Price and Rind (1992) with the emissions being distributed evenly between the convective cloud top height and the surface. The emissions are scaled so that the global total NO_x emission from lightning is 5 Tg (N) yr^{-1}. The NO_x emissions from civil and military aircraft are taken from NASA inventories for 1992 (Penner et al., 1999). The implementation of the emissions from aircraft is the same as for lightning with an annual total of 0.85 Tg(N) yr^{-1}.

The model dynamical scheme and depositional schemes have been tested extensively through comparisons with ^{222}Rn and other models (e.g. Stevenson et al., 1998) and were part of a major model inter-comparison study of the CO budget using 26 global chemistry transport models (Shindell et al., 2006). This inter-comparison showed that model transport schemes compared favourably with measurements and other models. The model stratosphere–troposphere exchange (Collins et al., 2003) and its ability to transport pollutants over a range of scales effectively (e.g. Derwent et al., 2004) has also been demonstrated. In addition, convection within the model has been extensively tested and validated (e.g. Collins et al., 1999, 2002). Therefore, in terms of transport and depositional loss (loss via OH for HCN is slow), the model is more than adequate for the intended study.

The biomass burning emissions for HCN are distributed as that of biomass burning emissions for CO with a single ratio used. The distribution is taken from the POET database; although there are several other distributions, we have not integrated them using other methods so that we can make a direct comparison with other model integrations by us. However, we do provide an analysis of uncertainty in the discussion section of this paper.

2.5 HCN

Using the biomass burning emission ratios derived in this work for HCN : CO (3.68×10^{-3}), the total emission of HCN via biomass burning introduced into the model was 0.92 Tg (N) yr^{-1}. HCN is removed by reaction with OH ($k = 1.2 \times 10^{-13} \exp(-400/T)$ cm^3 molecule^{-1} s^{-1}) and deposited into the ocean at a rate of 3.4×10^{-15} g (N) cm^{-2} s^{-1}. The model-derived lifetime for HCN is then ca. 3 months, consistent with other studies. Further simulations were carried out using more extreme ratios derived from other studies (e.g. 0.43×10^{-3}, which yields a total emission of 0.11 Tg (N) yr^{-1}, and 12.6×10^{-3}, which yields a total emission of 3.13 Tg (N) yr^{-1}). In addition to these three integrations, a second set of three, using the three HCN BB emission ratios relative to CO, was performed with a lower deposition velocity (halved) leading to an overall lifetime of ca. 6 months.

3 Aircraft measurements

In addition to HCN data, observations of CO and CH_3CN are also used in the analysis. CO data are reported at 1 Hz using a fast fluorescence CO analyser with an uncertainty of ±5 % (Gerbig et al., 1999). CH_3CN was measured by PTR-MS (see Murphy et al., 2010, for experimental details). During the BORTAS flights the PTR-MS measured selected VOCs with a cycle time of around 15 s. CH_3CN was measured at a m/z value of 42, which corresponds to the CH_3CNH^+ ion.

The BORTAS-B campaign was conducted between 12 July and 3 August 2011 based in Halifax, Canada. CIMS data from 5 flights during this campaign are presented here. Palmer et al. (2013) present an overview of the campaign with full descriptions of the operating area, all flights and fire activity maps. Figure 3 shows the flight paths and altitude of the aircraft for the data presented here.

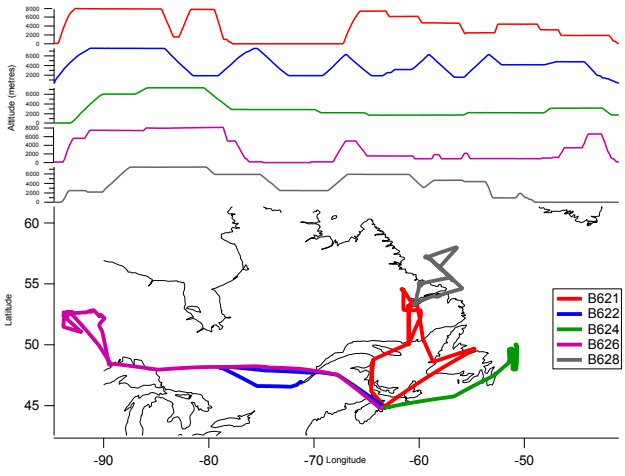

Fig. 3. The flight tracks from BORTAS-B from the CIMS data are presented here.

4 Biomass burning plume identification

HCN is a known BB tracer (Lobert et al., 1990), and CH_3CN is also an indicator of BB emissions, which is not significantly enhanced in areas of anthropogenic activity (de Gouw et al., 2003, 2006). These tracers and CO are regularly used to identify BB plumes, but a consistent method has not yet been established. Variation in background levels can make it difficult to define exactly when a plume is encountered without the aid of trace gas measurements which are not characteristic of BB fires. Hornbrook et al. (2011) defined a BB plume as having a CO mixing ratio above 175 ppbv, a CH_3CN mixing ratio of > 200 pptv and an HCN mixing ratio of > 400 pptv. When the background concentrations are low, the plumes selected are generally picked by enhancement above background. This method is likely to cause inaccuracies as there is no definite point at which "plume data" can be determined. Vay et al. (2011) limited the HCN mixing ratio to above 500 pptv, CO to above 160 ppbv and CH_3CN to above 225 pptv, but again they will experience similar issues with background concentrations. Simpson et al. (2011) state that the plume locations are defined by maximum CO concentrations. Holzinger et al. (2005) define a plume as CH_3CN concentrations increasing three standard deviations above neighbouring points.

Here we evaluate a statistical approach to plume identification by assuming that the threshold limit to define "in-plume" data is 10 times that of the standard deviation above the variation in the background (ICH-Q2B, 2009). The lifetime of HCN is long enough to allow plumes to be identified weeks away from the date of the fire. Dilution during this period will lower the concentrations, but there will still be a strong characteristic enhancement above the background levels, which will be analysed to evaluate if the normalised excess mixing ratio (NEMR) has been changed. The long-range transport and evolution of BB plumes can be evaluated using this method as the plume is not identified by a general enhancement for any air mass.

In order to define the plume, the median background concentration for each flight was calculated. Ten standard deviations were initially implemented as the threshold for "plume data". It was found that decreasing the number of standard deviations incrementally by 1 made no significant change in the NEMR (i.e. the NEMR was within error the same, and R^2 until 6 sigma). This threshold was therefore utilised to create a HCN to CO NEMR as this allowed the maximum number of data points to be implemented into the calculation. The difference between the slopes produced by the 6- and 10-sigma approach is within 2-sigma error and have similar R^2 values 0.72 and 0.67 respectively. The 6-sigma method reports a higher R^2 and utilises more data points in the calculation; therefore the 6-sigma approach is used for the analysis of flights B621, B622, B624, B626 and B628 as shown in Fig. 4. The HCN to CO ratios derived from the BORTAS flights are similar to those reported in the literature (Table 2). In order to evaluate this method, other possible approaches to BB plume identification were implemented using this data set. HCN, CO and CH_3CN have all been used in previous work (Vay et al., 2011; Hornbrook et al., 2011) to identify BB plumes. We have used 7 methods to define a plume: (1) 6 sigma above the HCN background, (2) 6 sigma above the CO background, (3) 6 sigma above the CH_3CN background, (4) above 100 ppb of CO, (5) above 300 ppt of HCN, (6) above 175 ppt of CH_3CN and 100 of ppb CO, and (7) above 200 ppb of CO. The HCN to CO NEMRs for each of the methods with the corresponding errors and R^2 value are shown in Table 3, and the percentage of data calculated to be in a plume is shown in Table 4.

The 6-sigma HCN method produced the highest average R^2 of 0.72. The methods using CO as a threshold exhibited low correlations on flight B628, as a result of a peak

Table 2. HCN : CO NEMRs as quoted in literature and the calculated NEMR for HCN from data collected throughout the BORTAS campaign, excluding flight B622. NEMR ratio units are ppt ppb^{-1}.

Lobert	Singh	Rinsland	Andreae	Sinha	Yokelson	Simpson	Hornbrook	This work
11.3 (lab)	0.001–0.011 (CA)	9.82 ± (AS)	0.43 ± 0.15 (Sv) 1.5 (TF) 1.4(TF)	9 ± 3 (Sv) 6 ± 2 (W) 9 ± 5 (G)	12.8 ± 9.5 (MC) 6.6 ± 4.8 (Yu) 7 ± 5.9 (TF)	8.2 ± 2 (Can)	8.8 ± 3.8 (As) 2.4 ± 0.9 (CA) 7.7 ± 3.2 (Can)	3.68 ± 0.149 (Can)

Sv: African savannas, TF: tropical forests, W: savanna woodland, G: savanna grassland, MC: Mexico City region, Yu: Yucatán, As: Asian, CA: California, Can: Canada, Lab: laboratory.

Table 3. The HCN : CO NEMRs (in pptv ppbv^{-1}) with R^2 of slope for 5 flights during BORTAS campaign calculated using varying methods previously described in literature.

	6-sigma HCN		6-sigma CO		6 sigma of CH3CN 6HCN : CO		100 ppb CO		300 ppt HCN		175 ppt CH3CN and 100 ppb CO		200 ppb CO	
	Slope	R^2	Slope	R^2	Slope	R^2	Slope	R^2	Slope	R^2	Slope	R^2	Slope	R^2
B621	4.70 ± 0.140	0.83	4.92 ± 0.114	0.83	4.75 ± 0.33	0.83	4.81 ± 0.105	0.85	5.03 ± 0.180	0.82	5.11 ± 0.147	0.84	5.81 ± 0.261	0.83
B622	0.66 ± 0.048	0.46	0.74 ± 0.030	0.62	0.85 ± 0.063	0.74	0.73 ± 0.033	0.59	0.40 ± 0.090	0.25	0.78 ± 0.039	0.61	0.69 ± 0.051	0.45
B624	2.68 ± 0.087	0.82	2.91 ± 0.111	0.76	3.24 ± 0.216	0.85	2.93 ± 1.254	0.72	2.72 ± 0.105	0.76	2.98 ± 0.141	0.70	3.13 ± 0.192	0.64
B626	2.72 ± 0.282	0.81	2.85 ± 0.222	0.83	2.83 ± 0.327	0.96	2.94 ± 0.150	0.83	2.97 ± 0.207	0.83	3.00 ± 0.402	0.81	2.64 ± 0.762	0.74
B628	3.68 ± 0.149	0.69	6.77 ± 0.30	0.60	0	0	6.21 ± 0.51	0.42	0.74 ± 0.330	0.24	4.66 ± 0.27	0.30	0	0
Average	2.89 ± 0.141	0.72	3.64 ± 0.156	0.73	2.33 ± 0.186	0.68	3.52 ± 0.186	0.68	2.37 ± 0.183	0.58	3.31 ± 0.309	0.65	2.45 ± 252	0.53

Table 4. Percentage of data determined to be within a plume from the BORTAS flights using varying possible plume identification methods.

% data in plume							
Flight	6-sigma HCN	6-sigma CO	6-sigma CH_3CN	100 ppb CO	300 ppt HCN	175 ppt CH_3 Cn and 100 ppb CO	200 ppb CO
B621	25.05	38.60	22.35	43.28	16.65	39.00	11.00
B622	46.80	83.47	62.51	73.40	12.31	51.00	49.00
B624	58.25	64.92	55.23	61.07	49.42	49.00	37.00
B626	13.71	22.12	13.89	48.23	24.22	8.00	3.00
B626	46.49	63.65	0	48.52	2.52	12.00	0.00
Average	38.06	54.44	30.80	54.90	21.02	31.80	20.00

in CO during low-level sections of the flight, as shown in Fig. 5. This can be attributed to non-BB sources of CO enhancing the CO levels where no HCN sources were present, as CO is known to have other natural and anthropogenic sources (Logan et al., 1981). This highlights a potential problem when using CO as a marker, as other measurements are required in order to determine the source. B622 had low CO concentrations but did show structure which was reciprocated by the HCN measurements. The CH_3CN data were too close to the detection limit during flight B628 to be able to determine a 6 sigma above background. The 200 ppb CO threshold approach removed all of these data from this flight, which would suggest that none of the flight encountered a BB plume. The method previously used by Hornbrook et al. (2011) produced an R^2 of 0.30 for this flight as a result of the low CO and CH_3CN concentrations, whereas the 6-sigma HCN approach produced an R^2 of 0.69. Using CO as a BB marker is limited due to the variability in sources of CO. This method can be used for relatively fresh and unmixed plumes, whereas aged plumes may suffer from enhancements of CO from other sources.

The methods using CH_3CN data did produce a high R^2 on many flights, as shown in Table 3. However, the limit of detection (LOD) of the PTR-MS to CH_3CN during BORTAS was a factor of 2.5 worse than the LOD of the CIMS towards HCN. As a result when sampling aged (and hence diluted) plumes, the S/N ratio is not significant enough to identify a plume, as exemplified by flight B628. Furthermore, as the PTR-MS was used to detect a range of compounds during each flight, the time response was slower than that of the CIMS system. As a result, the CH_3CN data have a time average from 9 to 20 s, depending on the number of target gases that were being measured. With this particular sampling protocol, it is difficult to measure accurately plumes close to the source as the lower measurement frequency may struggle to pick up small plumes as a result of the speed of the aircraft. Nevertheless, CH_3CN can be used to detect a BB plume accurately, under most conditions, as exemplified by flight B626.

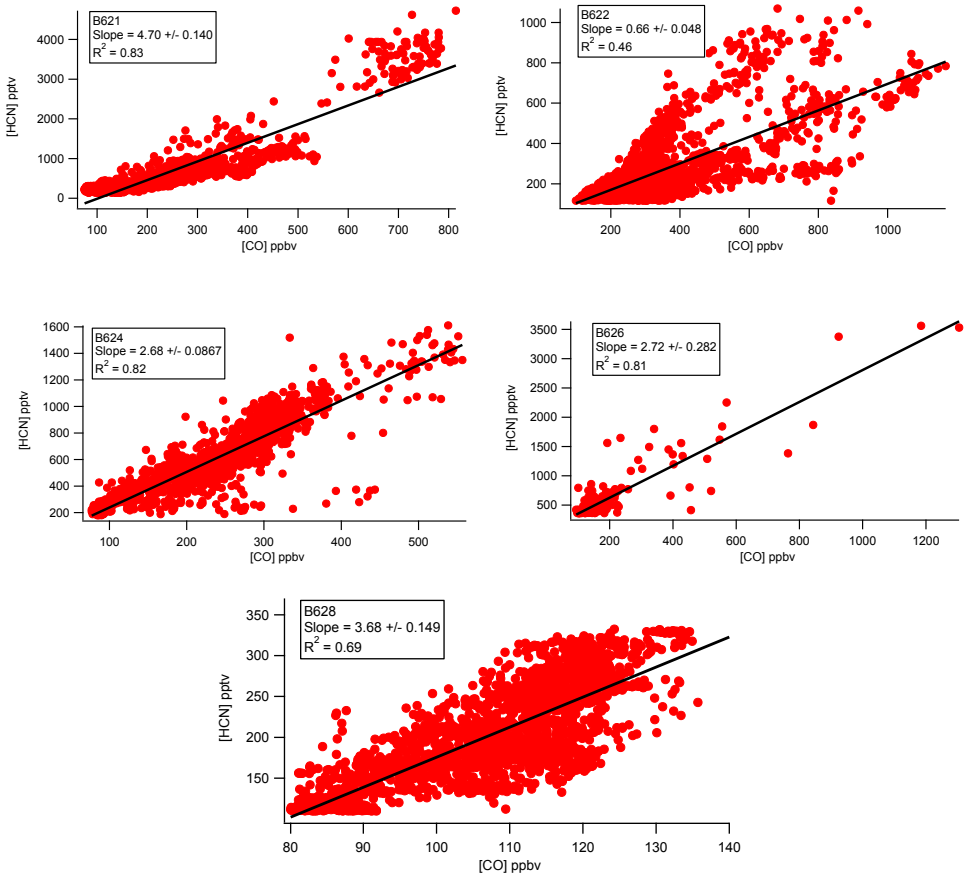

Fig. 4. HCN : CO correlations in plume determined by the 6-sigma HCN approach for 5 flights during the BORTAS campaign.

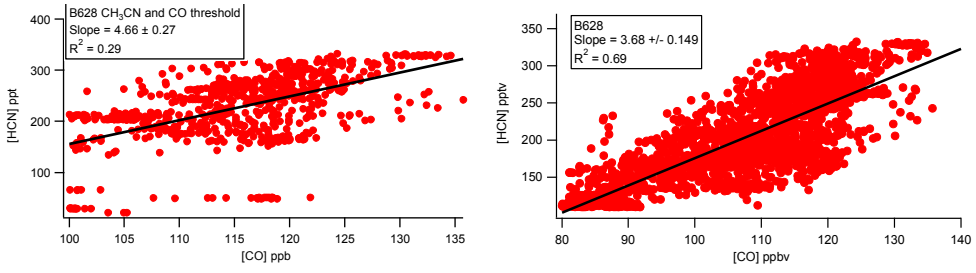

Fig. 5. In plume HCN : CO ratio from flight B628 using the 6-sigma HCN approach and the 175 ppt CH_3CN and 100 ppb CO thresholds.

Figure 6 displays an altitudinal profile performed in clean air from flight B622. An average concentration of 45 pptv is observed to remain fairly constant up to an altitude of 6000 m. The concentration then rises at 6000 m to a maximum of 111 pptv at 7000 m. Figure 7 represents the whole data set from flight B622 exhibiting stratification between atmospheric layers. There is clear evidence of BB plumes as a function of altitude, providing further evidence of the preservation of distinct BB plumes. Further investigation into the variance of NEMRs with altitude shows that all separate plumes' NEMRs lie within 2 standard deviations when plotted against the altitude at which they were intercepted. The biomass-burning-influenced plumes detected throughout the campaign ranged from 1 to 11 days old when the photochemical age is calculated. Mixing with fossil-fuel-influenced air masses would change the HCN : CO NEMR, although a high average HCN : CO R^2 correlation coefficient of 0.86 indicates that these plumes have not been influenced by fossil fuel plumes from North America.

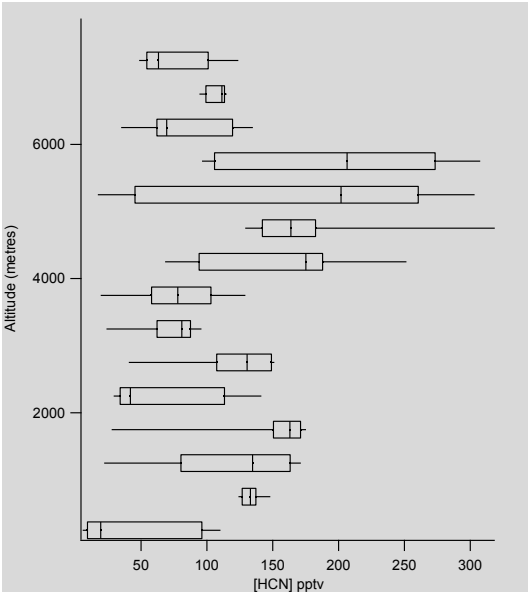

Fig. 6. All flight data for HCN from flight B622 plotted against altitude.

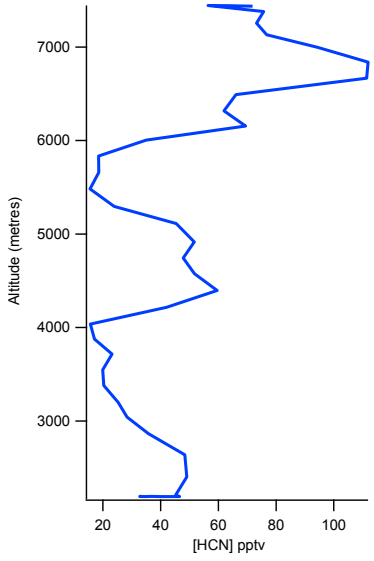

Fig. 7. Altitudinal profile performed during flight B622 in "clean air".

Figure 8, presenting all HCN data used to calculate an average NEMR, exhibits a change in gradient half way along the axis, possibly due to the higher HCN : CO ratio observed in flight B621. This outbound transit flight intercepted a strongly enhanced plume to the east of the Gulf of Saint Lawrence between 4 km and 7 km. This enhancement was observed throughout an altitudinal descent until 2 km, where another layer of BB is encountered. Back trajectories for this flight (discussed further in O'Shea et al., 2013) confirm the

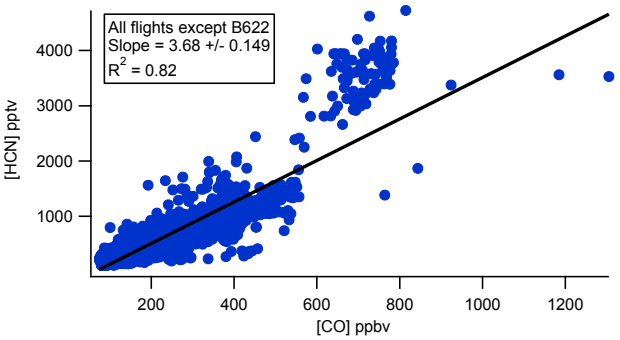

Fig. 8. HCN : CO correlations within BB plumes from the BORTAS campaign as determined using the 6-sigma HCN approach. Flight B622 data have been excluded due to the possible two separate slopes observed.

air mass passed over northwest Ontario, although it may have also been influenced further afield in areas such as northern Alberta and the Northwest Territories, possibly explaining the slight non-linear fit observed in Fig. 8, indicating a degree of mixing during this flight. Acetylene (C_2H_2) data also follow the same structure that HCN, CO and black carbon exhibit.

5 Emission ratios

The 6-sigma technique is used here to calculate the emission ratio of HCN from 4 flights during the BORTAS campaign 2011. Figure 8 shows all the data points which are used to calculate the mean NEMR: 3.68 ± 0.149 pptv ppbv^{-1}. The NEMR was calculated using the equation

$$\mathrm{NEMR} = \frac{\Delta[X]_{\mathrm{plume}} - [X]_{\mathrm{background}}}{[\mathrm{CO}]_{\mathrm{plume}} - [\mathrm{CO}]_{\mathrm{background}}}. \quad (1)$$

The data from flight B622 were omitted from this calculation due to the possible ageing and mixing of the plume. The NEMRs calculated during BORTAS are similar to those found in previous work, as seen in Table 2. The NEMRs reported in previous work vary from 0.43 to 12.8 pptv ppb^{-1}. The NEMR calculated here for HCN from Canadian BB plumes is lower than that found by Simpson et al. (2011), 8.2 pptv^{-1} ppb^{-1}. Hornbrook (2011) highlights the observed variation in the ratios, and offers a possible explanation for the difference between these NEMRs, but this variation is not seen from flight to flight during the BORTAS campaign, which measured both fresh plumes and aged plumes. Californian fire emission ratios during ARCTAS-CARB were significantly lower than the Canadian and Asian fires (Hornbrook et al., 2011), ranging from 2.4 ± 0.9 to 8.8 ± 3.8 pptv ppbv^{-1} respectively. Using the NEMRs calculated by Hurst et al. (2001), Hornbrook et al. (2011) report the low ratio of 0.43 pptv ppbv^{-1} originating from African savannas, tropical forests and extratropical forests, whereas

Yokelson et al. (2007b) reported a ratio in the Mexico City region of 12 ± 7 pptv ppbv^{-1}. The increase in these ratios may be attributed to the high NO_x levels found around Mexico City. Although emissions of HCN from motor vehicles are not believed to be important on a global scale, localised emissions may become significant (Crounse et al., 2009). Boreal forests are the primary source of fires in Canada, whereas Californian fires may be a result of varying fuels, such as coniferous forests and grass and shrubs (Hornbrook et al., 2011).

The 6-sigma HCN method of identifying BB plumes has shown the veracity of HCN as a BB-influenced plume marker. In addition, this method performed better than the others over the BORTAS campaign, as indicated by the statistics presented. Also, the 6-sigma HCN method showed the ability to define BB plumes accurately in air masses which had a low HCN background, enabling the identification of BB plumes in air masses distant from sources that were not constrained by a set threshold concentration. For example, a plume may have dispersed over large distances, lowering the concentration below the limit that defines a plume using previous methods. Nonetheless, this 6-sigma technique is still able to identify these plumes, as they are defined relative to the background. This 6-sigma method also has the same ability to determine VOC to CO ratios with the percentage of data at a high time resolution (3 s). This method is therefore used to determine a HCN to CO ratio for models to calculate a global HCN budget.

6 Model results

The purpose of the model integrations was to inspect the global HCN levels generated using the extreme HCN biomass ratios (relative to CO) reported in the literature and the value determined in this study, using two ocean deposition velocities that lead to HCN lifetimes of ca. 3 months and ca. 6 months. It should be noted that the variation in emission ratio reported in the literature is not in question here. There are myriad reasons for the variation in terms of vegetation type, temperature of the burn, etc. It is also noted that the limited available field measurements make comparison and constraint of the model somewhat limited. However, as we hope to show, the model results are instructive. The model results are in line with basic expectations: as the emission ratio increases, the global HCN level increases; when the deposition velocity is decreased, the global HCN for all three integrations also increases. Model results are presented in Fig. 9, which shows yearly averaged latitude–altitude profiles. Given the overall uncertainties, it is not justified to present more detailed seasonal results. We have deliberately used one HCN / CO ratio to distribute HCN emissions in these model runs to simplify them. We are not trying to reproduce any field data, but we can compare with measurements and of course compare between the integrations performed in a straightforward manner. If we assume the lower deposition velocity leading to a lifetime of about 6 months, we observe that an emission ratio of 0.4×10^{-3} leads to a global yearly averaged HCN level of 10–20 ppt. An emission ratio of 12.6×10^{-3} leads to a global yearly averaged HCN level of 300–600 ppt, and an emission ratio of 3.7×10^{-3} leads to a global yearly averaged HCN level of 80–180 ppt. In each case the highest levels are observed over the tropical regions, obviously driven by high biomass burning, with little variation in vertical structure, reflecting the surface deposition process dominating loss and leading to a sink in the Southern Hemisphere in the model.

There is no attempt here to reproduce field measurements, but it is instructive to compare field data with the model. We have concentrated on lower and mid-tropospheric measurements and note that there are measurements in the upper troposphere and lower stratosphere. Liang et al. (2007) observed HCN using aircraft during INTEX-A (July–August 2004). This field campaign ranged across the USA and Canada and took in measurements in both the Pacific and Atlantic oceans. Although very high levels were detected in biomass burning plumes (1090 ± 850 ppt), the background levels observed were 290 ± 70 ppt. In their comparison, Liang et al. (2007) reported levels in Asian plumes of 420 ± 60 ppt compared with 270 ± 80 ppt returned by Jacob et al. (2003) during Trace-P. Notholt et al. (2000) conducted vertical column measurements of HCN and other gases between 57° N and 45° S across the central Atlantic. HCN was detectable between 30° N and 30° S, with column amounts retrieved between 0 and 12 km. The HCN column amounts ranged from 100 to 220 ppt, with the maximum occurring just south of the Equator (10–15° S). Singh et al. (2003) report HCN levels of around 250 ± 150 pptv for HCN in February to April, and Ambrose et al. (2012) and Rinsland et al. (2007) report mean mixing ratios of 360 ppt and 220 ppt respectively, while Knighton et al. (2009) report a concentration ranging from 100 to 600 ppt and a mean background of 200 ppt. Therefore, based on the available measurements discussed thus far, we would conclude that yearly averaged levels of HCN vary between approximately 100 and 450 ppt in the lower to mid-troposphere. In the upper troposphere lightning may well contribute an additional non-negligible source, and this region will be impacted by continental-scale plumes, evidenced by a variety of measurements (e.g. Liang et al., 2007; Singh et al., 2007; Park et al., 2008; Randel et al., 2010; Wiegele et al., 2012). These plumes will contain a mixture of potential sources of HCN, of which biomass burning may well be the most predominant. It is also recognised that emission ratios will vary for different types of biomass burning, depending on vegetation type, temperature of burn, etc. No one ratio will be representative of the global emission. However, inspection of the model integrations suggests that the extreme ratios returned from field measurements are indeed extreme values: adopting a uniform ratio of 0.4×10^{-3} returns a globally averaged HCN that is far

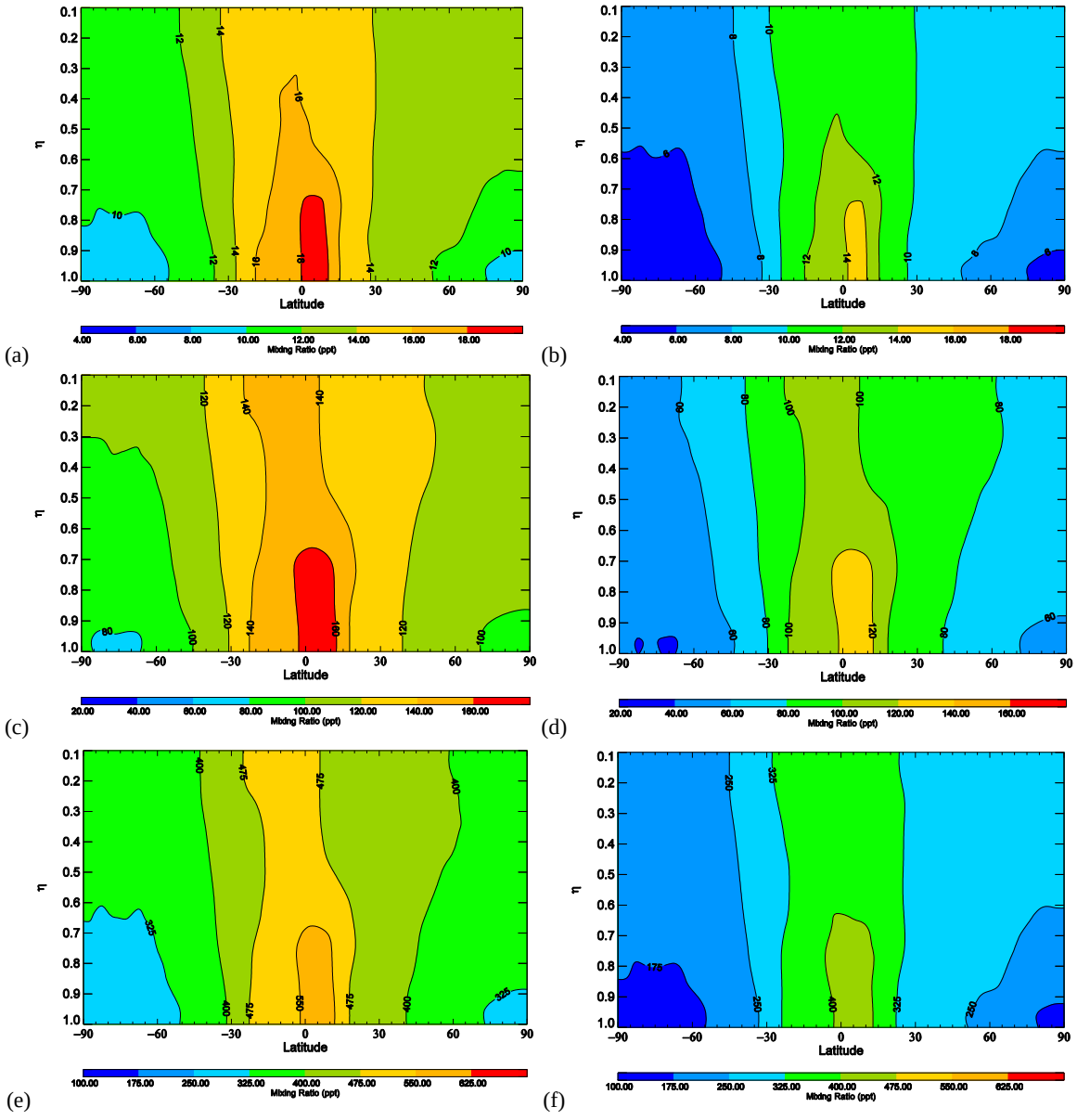

Fig. 9. Yearly average HCN derived from model integrations with two ocean deposition velocities leading to a lifetime of 3 months and 6 months. **(a)** Emission ratio (HCN : CO) of 4×10^{-4} ppb ppb^{-1} and a lifetime with respect to deposition of 3 months. **(b)** Emission ratio of 4×10^{-4} and a lifetime with respect to deposition of 6 months. **(c)** Emission ratio of 3.7×10^{-3} and a lifetime with respect to deposition of 3 months. **(d)** Emission ratio of 3.7×10^{-3} and a lifetime with respect to deposition of 6 months. **(e)** Emission ratio of 12×10^{-3} and a lifetime with respect to deposition of 3 months. **(f)** Emission ratio of 12×10^{-3} and a lifetime with respect to deposition of 6 months.

too low, irrespective of whether the lifetime is 3 or 6 months. Similarly, adopting a ratio of 12.6×10^{-3} produces HCN levels that have been observed but they are somewhat higher than expected for a yearly average, given the background measurements made. Using the ratio derived in this study as a global value produces HCN levels that are reasonable, compared with available field measurements, but are an underestimate. An underestimate is completely consistent with the fact that more influential biomass burning regions have returned a higher HCN : CO ratio. The satellite-derived measurements of Wiegle et al. (2012), although restricted in altitude to above 5 km, suggest strongly that biomass burning (particularly that located in the Southern Hemisphere) is a dominant source and lends confidence to the present broad brush model comparisons with measurements. Vegetation has also been suggested as a non-negligible source of HCN (e.g. Fall et al., 2001), and vertical profile data from the Jungfraujoch station in Switzerland (Rinsland et al., 2000)

Table 5. Estimated CO emission totals from biomass burning in $Tg\,yr^{-1}$. * Totals reported following the analysis of Stroppiana et al. (2010).

Total ($Tg\,yr^{-1}$)	Source	Reference
720	inventory	Andreae and Merlet (2001)
1422	VGT inventory	Liousse et al. (2010)*
548	ATSR inventory	Mieville et al. (2010)*
770	MODIS inventory	Chin et al. (2002)*
365	GFED3 inventory	Van der Werf et al. (2010)*
594	MOPITT inventory	Pétron et al. (2004)
270	Model derived	Taylor et al. (1996)
507	Model comparison	Shindell et al. (2006)
494	POET inventory	Granier et al. (2005)

suggest that, in addition to biomass burning, there may well be a significant direct emission from vegetation.

It is clear that the depositional velocity adopted for HCN is crucial in any budget analysis, and for the ones used in this study increasing the lifetime of HCN from ca. 3 months to 6 months increases model HCN levels by a factor of ~ 1.4, irrespective of the emission ratio used. In this integration the CO biomass burning total used is $\sim 500\,Tg\,yr^{-1}$. There are a range of estimates for this total summarised in Table 5.

There is a wide range of estimates, but the majority lie between $750\,Tg\,yr^{-1}$ and $350\,Tg\,yr^{-1}$. Therefore to a first approximation the model-estimated HCN levels will vary by a factor of 1.5 based on the CO emission uncertainty alone. HCN : CO biomass burning emission ratios will vary with type of burn and vegetation and are summarised in Table 5. Note that this ratio will vary with vegetation type and that using one ratio is not physically correct. However, the range reported has allowed us to investigate in a simple way the impact of these ratios on atmospheric levels.

In summary, model integrations suggest that the extreme ratios reported in the literature generate too little or too much HCN and really are extreme values. Using the ratios reported in this study to drive the model emissions produces HCN levels that are an underestimate compared with a range of field measurements, which are consistent with the fact that higher ratios are seen in tropical biomass burning events for example. However, the model integrations highlight that depositional loss is very important to determining HCN atmospheric background levels and that further work is required to constrain this loss process. In addition, more atmospheric measurements are welcome, particularly vertical column and transects.

7 Conclusions

A CIMS instrument was developed for the airborne measurement of HCN in the lower atmosphere using methyl iodide as the ionisation reagent gas. HCN measurements were successfully attained over Canada in July and August 2011, during the BORTAS-B 2011 campaign on board the FAAM BAe-146 aircraft. The high sensitivity (4 ± 0.9 ion counts $s^{-1}\,pptv^{-1}$), low limit of detection (5 pptv) and selectivity of the data acquired and presented here with a time resolution of 3 s illustrate the ability of this instrument to measure HCN with a high precision; it is, therefore, a highly sophisticated instrument for detecting BB-influenced plumes. The mixing ratios measured through the BB-influenced plumes ranged from 0.67 to 5.2 ppb covering the range of previously reported atmospheric levels (Singh et al., 2003, 2012; Knighton et al., 2009) and were strongly correlated with CO and CH_3CN, strengthening the ability of HCN to be a unique marker for biomass burning.

The 6-sigma methodology implemented and tested here for plume definition has been shown to produce the strongest correlation with CO, indicating that it is potentially an excellent method for defining biomass burning plumes. The NEMR (relative to CO) calculated using this plume identification method was $3.68 \pm 0.149\,pptv\,ppbv^{-1}$, which is in the range of previously reported values (Andreae et al., 2001; Sinha et al., 2003; Yokelson et al., 2009; Hornbrook et al., 2011) indicating the precision of the HCN measurements. The study-averaged NEMR was then used to estimate the total emission of HCN via biomass burning, which was calculated to be $0.91\,Tg\,(N)\,yr^{-1}$.

These first results of HCN measurements by CIMS using I^- chemistry show the capability of CIMS to attain high-frequency HCN measurements in the lower atmosphere with a high sensitivity and low limit of detection. The data produced also show the accuracy at which HCN measurements can define biomass burning plumes and the reliability of this method.

Acknowledgements. The authors would like to thank everyone involved with the BORTAS project. C. J. Percival and D. E. Shallcross thank NERC, under whose auspices various elements of this work were carried out.

Edited by: S. Matthiesen

References

Akagi, S. K., Yokelson, R. J., Wiedinmyer, C., Alvarado, M. J., Reid, J. S., Karl, T., Crounse, J. D., and Wennberg, P. O.: Emission factors for open and domestic biomass burning for use in atmospheric models, Atmos. Chem. Phys., 11, 4039–4072, doi:10.5194/acp-11-4039-2011, 2011.

Akagi, S. K., Yokelson, R. J., Burling, I. R., Meinardi, S., Simpson, I., Blake, D. R., McMeeking, G. R., Sullivan, A., Lee, T., Kreidenweis, S., Urbanski, S., Reardon, J., Griffith, D. W. T., Johnson, T. J., and Weise, D. R.: Measurements of reactive trace gases and variable O_3 formation rates in some South Carolina biomass burning plumes, Atmos. Chem. Phys., 13, 1141–1165, doi:10.5194/acp-13-1141-2013, 2013.

Ambrose, J. L., Zhou, Y., Haase, K., Mayne, H. R., Talbot, R., and Sive, B. C.: A gas chromatographic instrument for measurement of hydrogen cyanide in the lower atmosphere, Atmos. Meas. Tech., 5, 1229–1240, doi:10.5194/amt-5-1229-2012, 2012.

Amiro, B. D., Cantin, A., Flannigan, M. D., and de Groot, W. J.: Future emissions from Canadian boreal forest fires, Can. J. For. Res., 39, 383–395, 2009.

Andreae, M. O. and Merlet, P.: Emission of trace gases and aerosols from biomass burning, Global Biogeochem. Cy., 15, 955–966, doi:10.1029/2000GB001382, 2001.

Archibald, A. T., Cooke, M. C., Utembe, S. R., Shallcross, D. E., Derwent, R. G., and Jenkin, M. E.: Impacts of mechanistic changes on HO_x formation and recycling in the oxidation of isoprene, Atmos. Chem. Phys., 10, 8097–8118, doi:10.5194/acp-10-8097-2010, 2010.

Bange, H. W. and Williams, J.: New directions: Acetonitrile in atmospheric and biogeochemical cycles, Atmos. Environ., 34, 4959–4960, 2000.

Becidan, M., Skreiberg, Ø., and Hustad, J. E.: NO_x and N_2O precursors (NH3 and HCN) in pyrolysis of biomass residues, Energy and Fuels, 21, 1173–1180, 2007.

Bertschi, I. T., Yokelson, R. J., Ward, D. E., Christian, T. J., and Hao, W. M.: Trace gas emissions from the production and use of domestic biofuels in Zambia measured by open-path Fourier transform infrared spectroscopy, J. Geophys. Res., 08, 8469, doi:10.1029/2003JD004402, 2003.

Boldi, R. A.: A Model of the Ion Chemistry of Electrified Convection. Ph.D. Thesis MIT, USA, http://dspace.mit.edu/handle/1721.1/51502 (last access: September 2012), 1993.

Chin, M., Ginoux, P., Kinne, S., Torres, O., Holben, B. N., Duncan, B. N., Martin, R. V., Logan, J. A., Higurashi, A., and Nakajima, T.: Tropospheric Aerosol Optical Thickness from the GOCART Model and Comparisons with Satellite and Sun Photometer Measurements, J. Atmos. Sci., 59, 461–483, 2002.

Christian, T. J., Kleiss, B., Yokelson, R. J., Holzinger, R., Crutzen, P. J., Hao, W. M., Shirai, T., and Blake, D. R.: Comprehensive laboratory measurements of biomass-burning emissions: 2. First intercomparison of open-path FTIR, PTR-MS, and GC-MS/FID/ECD, J. Geophys.Res., 109, D02311, doi:10.1029/2003JD003874, 2004.

Christian, T. J., Yokelson, R. J., Cárdenas, B., Molina, L. T., Engling, G., and Hsu, S.-C.: Trace gas and particle emissions from domestic and industrial biofuel use and garbage burning in central Mexico, Atmos. Chem. Phys., 10, 565–584, doi:10.5194/acp-10-565-2010, 2010.

Cicerone, R. J. and Zellner, R.: The atmospheric chemistry of hydrogen cyanide (HCN), J. Geophys. Res., 88, 10689–10696, 1983.

Coffey, M. T., Mankin, W. G., and Cicerone, R. J.: Spectroscopic detection of stratospheric hydrogen cyanide, Science, 214, 333–335, 1981.

Colarco, P. R., Schoeberl, M. R., Doddridge, B. G., Marufu, L. T., Torres, O., and Welton, E. J.: Transport of smoke from Canadian forest fires to the surface near Washington DC: injection height, entrainment, and optical properties, J. Geophys. Res., 109, D06203, doi:10.1029/2003JD004248, 2004.

Collins, W. J., Stevenson, D. S., Johnson, C. E., and Derwent, R. G.: Role of convection in determining the budget of odd hydrogen in the upper troposphere, J. Geophys. Res., 104, 26927–26942, doi:10.1029/1999JD900143, 1999.

Collins, W., Stevenson, D., Johnson, C., and Derwent, R.: Tropospheric ozone in a global-scale three-dimensional Lagrangian model and its response to NO_x emission controls, J. Atmos. Chem., 26, 223–274, 1997.

Collins, W. J., Derwent, R. G., Johnson, C. E., and Stevenson, D. S.: A comparison of two schemes for the convective transport of chemical species in a Lagrangian global chemistry model, Q. J. Roy. Meteorol. Soc., 128, 991–1009, doi:10.1256/0035900021643629, 2002.

Collins, W. J., Derwent, R. G., Garnier, B., Johsnon, C. E., Sanderson, M. G., and Stevenson, D. S.: Effect of stratosphere-troposphere exchange on the future tropospheric ozone trend, J. Geophys. Res. Atmos., 108, 8528, doi:10.1029/2002JD002617, 2003.

Cooke, M. C., Utembe, S. R., Archibald, A. T., Jenkin, M. E., Derwent, R. G., and Shallcross, D. E.: Using a reduced Common Representative Intermediates (CRIv2-R5) Mechanism to Simulate Tropospheric Ozone in a 3-D Lagrangian Chemistry Transport Model, Atmos. Environ., 44, 1609–1622, 2010a.

Cooke, M. C., Utembe, S. R., Carbajo, P. G., Archibald, A. T., Orr-Ewing, A. J., Derwent, R. G., Jenkin, M. E., and Shallcross, D. E.: Impacts of Formaldehyde Photolysis Rates on Tropospheric Chemistry, Atmos. Sci. Lett., 11, 33–38, 2010b.

Cooke, M. C., Marven, A. R., Utembe, S. R., Archibald, A. R., Ensor, G. W. R., Jenkin, M. E., Derwent, R. G., O'Doherty, S. J., and Shallcross, D. E.: On the effect of a global adoption of various fractions of biodiesel on key species in the troposphere, Int. J. Oil, Gas and Coal Tech., 3, 88–103, 2010c.

Crounse, J. D., McKinney, K. A., Kwan, A. J., and Wennberg, P. O.: Measurement of gas-phase hydroperoxides by chemical ionization mass spectrometry, Anal. Chem., 78, 6726–6732, doi:10.1021/ac0604235, 2006.

Crounse, J. D., DeCarlo, P. F., Blake, D. R., Emmons, L. K., Campos, T. L., Apel, E. C., Clarke, A. D., Weinheimer, A. J., McCabe, D. C., Yokelson, R. J., Jimenez, J. L., and Wennberg, P. O.: Biomass burning and urban air pollution over the Central Mexican Plateau, Atmos. Chem. Phys., 9, 4929–4944, doi:10.5194/acp-9-4929-2009, 2009.

Damoah, R., Spichtinger, N., Forster, C., James, P., Mattis, I., Wandinger, U., Beirle, S., Wagner, T., and Stohl, A.: Around the world in 17 days – hemispheric-scale transport of forest fire smoke from Russia in May 2003, Atmos. Chem. Phys., 4, 1311–1321, doi:10.5194/acp-4-1311-2004, 2004.

de Gouw, J. A., Warneke, C., Parrish, D. D., Holloway, J. S., Trainer, M., and Fehsenfeld, F. C.: Emission sources and ocean uptake of acetonitrile (CH_3CN) in the atmosphere, J. Geophys. Res., 108, 4329, doi:10.1029/2002JD002897, 2003.

de Gouw, J. A., Warneke, C., Stohl, A., Wollny, A. G., Brock, C. A., Cooper, O. R., Holloway, J. S., Trainer, M., Fehsenfeld, F. C., Atlas, E. L., Donnelly, S. G., Stroud, V., and Lueb, A.: Volatile organic compounds composition of merged and aged forest fire plumes from Alaska and Western Canada, J. Geophys. Res., 111, D10303, doi:10.1029/2005JD006175, 2006.

Derwent, R. G., Stevenson, D. S., Collins, W. J., and Johnson, C. E.: Intercontinental transport and the origins of the ozone observed at surface sites in Europe, Atmos. Environ., 38, 1891–1901, doi:10.1016/j.atmosenv.2004.01.008, 2004.

Derwent, R. G., Stevenson, D. S., Doherty, R. M., Collins, W. J., Sanderson, M. G., and Johnson, C. E.: Radiative forcing from surface NO_x emissions: spatial and seasonal variations, Climatic Change, 88, 385–401, 2008.

Fall, R., Custer, T. G., Kato, S., and Bierbaum, V. M.: The biogenic acetne-HCN connection, Atmos. Environ., 35, 1713–1714, 2001.

Flannigan, M. D., Logan, K. A., Amiro, B. D., Skinner, W. R., and Stocks, B. J.: Future area burned in Canada, Clim. Change, 72, 1–16, 2005.

Fromm, M., Alfred, J., Hoppel, K., Hornstein, J., Bevilacqua, R., Shettle, E., Servranckx, R., Li, Z. Q., and Stocks, B.: Observations of boreal forest fire smoke in the stratosphere by POAM III, SAGE II, and lidar in 1998, Geophys. Res. Lett., 27, 1407–1410, doi:10.1029/1999GL011200, 2000.

Gerbig, C., Schmitgen, S., Kley, D., and Volz-Thomas, A.: An improved fast-response vacuum UV resonance fluorescence CO instrument, J. Geophys. Res., 104, 1699–1704, 1999.

Gillett, N. P., Weaver, A. J., Zwiers, F. W., and Flannigan, M. D.: Detecting the effect of climate change on Canadian forest fires, Geophys. Res. Lett., 31, L18211, doi:10.1029/2004GL020876, 2004.

Glarborg, P., Jensen, A. D., and Johnsson, J. E.: Fuel nitrogen conversion in solid fuel fired systems, Prog. Energy Combust. Sci., 29, 89–113, 2003.

Goode, J. G., Yokelson, R. J., Ward, D. E., Susott, R. A., Babbitt, R. E., Davies, M. A., and Hao, W. M.: Measurements of excess O_3, CO_2, CO, CH_4, C_2H_4, C_2H_2, HCN, NO, NH_3, HCOOH,CH_3OOH, HCHO, and CH_3OH in 1997 Alaskan biomass burning plumes by airborn Fourier transform infrared spectroscopy (AFTIR), J. Geophys. Res., 105, 22147–22166, 2000a.

Goode, J. G., Yokelson, R. J., Susott, R. A., and Ward, D. E.: Trace gas emissions from laboratory biomass fires measured by open-path FTIR: Fires in grass and surface fuels, J. Geophys. Res., 104, 21237–21245, 2000b.

Granier, C., Lamarque, J., Mieville, A., Muller, J., Olivier, J., Orlando, J., Peters, J., Petron, G., Tyndall, S., and Wallens, S.: A Database of Surface Emissions of Ozone Precursors, available at: http://www.aero.jussieu.fr/projet/ACCENT/POET.php, last access: November 2012.

Holzinger, R., Warneke, C., Hansel, A., Jordan, A., and Lindinger, W.: Biomass burning as a source of formaldehyde, acetaldehyde, methanol, acetone, acetonitrile, and hydrogen cyanide, Geophys. Res. Lett., 26, 1161–1164, 1999.

Holzinger, R., Jordan, A. Hansel, A., and W. Lindinger, Automobile emissions of acetonitrile: Assessments of its contribution to the global source, Atmos. Environ., 38, 187–193, 2001.

Holzinger, R., Williams, J., Salisbury, G., Klüpfel, T., de Reus, M., Traub, M., Crutzen, P. J., and Lelieveld, J.: Oxygenated compounds in aged biomass burning plumes over the Eastern Mediterranean: evidence for strong secondary production of methanol and acetone, Atmos. Chem. Phys., 5, 39–46, doi:10.5194/acp-5-39-2005, 2005.

Hornbrook, R. S., Blake, D. R., Diskin, G. S., Fried, A., Fuelberg, H. E., Meinardi, S., Mikoviny, T., Richter, D., Sachse, G. W., Vay, S. A., Walega, J., Weibring, P., Weinheimer, A. J., Wiedinmyer, C., Wisthaler, A., Hills, A., Riemer, D. D., and Apel, E. C.: Observations of nonmethane organic compounds during ARCTAS – Part 1: Biomass burning emissions and plume enhancements, Atmos. Chem. Phys., 11, 11103–11130, doi:10.5194/acp-11-11103-2011, 2011.

Hurst, D. F., Griffith, D. W. T., and Cook, G. D.: Trace gas emissions from biomass burning in tropical Australian savannas, J. Geophys. Res., 99, 16441–16,456, 1994a.

Hurst, D. F., Griffith, D. W. T., and Cook, G. D.: Trace gas emissions from biomass burning in tropical Australian savannas, J. Geophys. Res., 99, 16441–16456, 1994b.

ICH-Q2B Validation of Analytical Procedure: Methodology, International Conference on Harmonisation of Technical Requirements for Registration of Pharmaceuticals for HUman Use, Geneva, Switzerland, p. 9, November 1996.

Jacob, D. J., Crawford, J. H., Kleb, M. M., Connors, V. S., Bendura, R. J., Raper, J. L., Sachse, G. W., Gille, J. C., Emmons, L., and Heald, C. L.: Transport and Chemical Evolution over the Pacific (TRACE-P) aircraft mission: Design, execution, and first results, J. Geophys. Res., 108, 9000, doi:10.1029/2002JD003276, 2003.

Jenkin, M. E., Watson, L. A., Utembe, S. R., and Shallcross, D. E.: A Common Representative Intermediates (CRI) mechanism for VOC degradation. Part 1: Gas phase mechanism development, Atmos. Environ., 42, 7185–7195, 2008.

Johnson, W. R. and Kang, J. C.: Mechanisms of hydrogen cyanide formation from the pyrolysis of amino acids and related compounds, J. Org. Chem., 36, 189–192, 1971.

Jost, H. J., Drdla, K., Stohl, A., Pfister, L., Loewenstein, M., Lopez, J. P., Hudson, P. K., Murphy, D. M., Cziczo, D. J., Fromm, M., Bui, T. P., Dean-Day, J., Gerbig, C., Mahoney, M. J., Richard, E. C., Spichtinger, N., Pittman, J. V., Weinstock, E. M., Wilson, J. C., and Xueref, I.: In-situ observations of mid-latitude forest fire plumes deep in the stratosphere, Geophys. Res. Lett. 31, 11101, doi:10.1029/2003GL019253, 2004.

Kasischke, E. S. and Turetsky, M. R.: Recent changes in the fire regime across the North American boreal region – Spatial and temporal patterns of burning across Canada and Alaska, Geophys. Res. Lett., 33, L09703, doi:10.1029/2006GL025677, 2006.

Kasischke, E. S., Hyer, E. J., Novelli, P. C., Bruhwiler, L. P., French, N. H. F., Sukhinin, A. I., Hewson, J. H., and Stocks, B. J.: Influences of boreal fire emissions on Northern Hemisphere atmospheric carbon and carbon monoxide, Global Biogeochem. Cy., 19, GB1012, doi:10.1029/2004GB002300, 2005.

Kleinböhl, A., Toon, G. C., Sen, B., Blavier, J.-F. L., Weisenstein, D. K., Strekowski, R. S., Nicovich, J. M., Wine, P. H., and Wennberg, P. O.: On the stratospheric chemistry of ydrogen cyanide, Geophys. Res. Lett., 33, L11806, doi:10.1029/2006GL026015, 2006.

Knighton, W. B., Fortner, E. C., Midey, A. J., Viggiano, A. A., Herndon, S. C., Wood, E. C., and Kolb, C. E.: HCN detection with a proton transfer reaction mass spectrometer, Int. J. Mass. Spectrom., 283, 112–121, 2009.

Le Breton, M., McGillen, M. R., Muller, J. B. A., Bacak, A., Shallcross, D. E., Xiao, P., Huey, L. G., Tanner, D., Coe, H., and Percival, C. J.: Airborne observations of formic acid using a chemical ionization mass spectrometer, Atmos. Meas. Tech., 5, 3029–3039, doi:10.5194/amt-5-3029-2012, 2012.

Levine, J. S.: Global biomass burning: a case study of the gaseous and particulate emissions released to the atmosphere during the 1997 fires in Kalimantan and Sumatra, Indonesia, in: Biomass Burning and its Inter-Relationships with the Climate System, edited by: Innes, J. L., Beniston, M., and Verstraete, M. M.,

Kluwar Academic Publishers, Boston, 15–31, 2000.

Li, Q. B., Jacob, D. J., Bey, I., Yantosca, R. M., Zhao, Y. J., Kondo, Y., and Notholt, J.: Atmospheric hydrogen cyanide (HCN): biomass burning source, ocean sink?, Geophys. Res.Lett., 27, 357–360, doi:10.1029/1999GL010935, 2000.

Li, Q., Jacob, D. J., Yantosca, R. M., Heald, C. L., Singh, H. B., Koike, M., Zhao, Y., Sachse, G. W., and Streets, D. G.: A global three-dimensional model analysis of the atmospheric budget of HCN and CH3CN: Constraints from aircraft and ground measurements, J. Geophys. Res., 108, 8827, doi:10.1029/2002JD003075, 2003.

Li, Q., Palmer, P. I., Pumphrey, H. C., Bernath, P., and Mahieu, E.: What drives the observed variability of HCN in the troposphere and lower stratosphere?, Atmos. Chem. Phys., 9, 8531–8543, doi:10.5194/acp-9-8531-2009, 2009.

Liang, Q., Jaegle, L., Hudman, R. C., Turquety, S., Jacob, D. J., Avery, M. A., Browell, E. V., Sachse, G. W., Blake, D. R., Brune, W., Ren, X., Cohen, R. C., Dibb, J. E., Fired, A., Fuelberg, H., Porter, M., Heikes, B. G., Huey, G., Singh, H. B., and Wennberg, P. O.: Summertime influence of Asian pollution in the free troposphere over North America. J. Geophys. Res., 112, D12S11, doi:10.1029/2006JD007919, 2007.

Liousse, C., Guillaume, B., Grégoire, J. M., Mallet, M., Galy, C., Pont, V., Akpo, A., Bedou, M., Castéra, P., Dungall, L., Gardrat, E., Granier, C., Konaré, A., Malavelle, F., Mariscal, A., Mieville, A., Rosset, R., Serça, D., Solmon, F., Tummon, F., Assamoi, E., Yoboué, V., and Van Velthoven, P.: Updated African biomass burning emission inventories in the framework of the AMMA-IDAF program, with an evaluation of combustion aerosols, Atmos. Chem. Phys., 10, 9631–9646, doi:10.5194/acp-10-9631-2010, 2010.

Lobert, J. M., Scharffe, D. H., Hao, W. M., and Crutzen, P. J.: Importance of biomass burning in the atmospheric budgets of nitrogen-containing gases, Nature, 346, 552–554, 1990.

Lobert, J. M., Scharffe, D. H., Kuhlbusch, T. A., Seuwen, R., and Crutzen, P. J.: Experimental evaluation of biomass burning emissions: Nitrogen and carbon containing compounds, in: Global Biomass Burning: Atmospheric, Climatic, and Biospheric Implications, edited by: Levine, J. S., MIT Press, Cambridge, Massachusetts, USA, 289–304, 1991.

Logan, J. A., Prather, M. J., Wofsy, S. C., and McElroy, M. B.: Tropospheric chemistry: A global perspective, J. Geophys. Res., 86, 7210–7254, 1981.

Mieville, A., Granier, C., Liousse, C., Guillaume, B., Mouillot, F., Lamarque, J.-F., Gregoire, J.-M., and Petron, G.: Emissions of gases and particles from biomass burning during the 20th century using satellite data and an historical reconstruction, Atmos. Environ., 44, 1469–1477, 2010.

Morris, G. A., Hersey, S., Thompson, A. M., Pawson, S., Nielsen, J. E., Colarco, P. R., McMillan, W. W., Stohl, A., Turquety, S., Warner, J., Johnson, B. J., Kucsera, T. L., Larko, D. E., Oltmans, S. J., and Witte, J. C.: Alaskan and Canadian forest fires exacerbate ozone 20 pollution over Houston, Texas, on 19 and 20 July 2004, J. Geophy. Res., 111, D24S03, doi:10.1029/2006JD007090, 2006.

Murphy, J. G., Oram, D. E., and Reeves, C. E.: Measurements of volatile organic compounds over West Africa, Atmos. Chem. Phys., 10, 5281–5294, doi:10.5194/acp-10-5281-2010, 2010.

Notholt, J., Toon, G. C., Rinsland, C. P., Pougatchev, N. S., Jones, N. B., Connor, B. J., Weller, R., Gautrois, M., and Schrems, O.: Latitudinal variations of trace gas concentrations in the free troposphere measured by solar absorption spectroscopy during a ship cruise, J. Geophys. Res., 105, 1337–1349, 2000.

Nowak, J. B., Neuman, J. A., Kozai, K., Huey, L. G., Tanner, D. J., Holloway, J. S., Ryerson, T. B., Frost, G. J., McKeen, S. A., and Fehsenfeld, F. C.: A chemical ionization mass spectrometry technique for airborne measurements of ammonia, J. Geophys. Res.-Atmos., 112, D10S02, doi:10.1029/2006JD007589, 2007.

O'Shea, S. J., Allen, G., Gallagher, M. W., Bauguitte, S. J.-B., Illingworth, S. M., Le Breton, M., Muller, J. B. A., Percival, C. J., Archibald, A. T., Oram, D. E., Parrington, M., Palmer, P. I., and Lewis, A. C.: Airborne observations of trace gases over boreal Canada during BORTAS: campaign climatology, airmass analysis and enhancement ratios, Atmos. Chem. Phys. Discuss., 13, 14069–14114, doi:10.5194/acpd-13-14069-2013, 2013.

Palmer, P. I., Parrington, M., Lee, J. D., Lewis, A. C., Rickard, A. R., Bernath, P. F., Duck, T. J., Waugh, D. L., Tarasick, D. W., Andrews, S., Aruffo, E., Bailey, L. J., Barrett, E., Bauguitte, S. J.-B., Curry, K. R., Di Carlo, P., Chisholm, L., Dan, L., Forster, G., Franklin, J. E., Gibson, M. D., Griffin, D., Helmig, D., Hopkins, J. R., Hopper, J. T., Jenkin, M. E., Kindred, D., Kliever, J., Le Breton, M., Matthiesen, S., Maurice, M., Moller, S., Moore, D. P., Oram, D. E., O'Shea, S. J., Christopher Owen, R., Pagniello, C. M. L. S., Pawson, S., Percival, C. J., Pierce, J. R., Punjabi, S., Purvis, R. M., Remedios, J. J., Rotermund, K. M., Sakamoto, K. M., da Silva, A. M., Strawbridge, K. B., Strong, K., Taylor, J., Trigwell, R., Tereszchuk, K. A., Walker, K. A., Weaver, D., Whaley, C., and Young, J. C.: Quantifying the impact of BOReal forest fires on Tropospheric oxidants over the Atlantic using Aircraft and Satellites (BORTAS) experiment: design, execution and science overview, Atmos. Chem. Phys. Discuss., 13, 4127–4181, doi:10.5194/acpd-13-4127-2013, 2013.

Park, M., Randel, W. J., Emmons, L. K., Bernath, P. F., Walker, K. A., and Boone, C. D.: Chemical isolation in the Asian monsoon anticyclone observed in Atmospheric Chemistry Experiment (ACE-FTS) data, Atmos. Chem. Phys., 8, 757–764, doi:10.5194/acp-8-757-2008, 2008.

Penner, J. E., Lister, D. H., Griggs, D. J., Dokken, D. J., and McFarland, M.: IPCC Special Report on Aviation and the Global Atmosphere. Technical report, tech.rep., the IPCC, Cambridge University Press, Cambridge, UK and New York, NY, USA, 365 pp., 1999.

Petron, G., Granier, C., Khattatov, B., Yudin, V., Lamarque, J.-F., Emmons, L., Gille, J., and Edwards, D. P.: Monthly CO surface sources inventory based on the 2000–2001 MOPITT satellite data, Geophys. Res. Lett., 31, L21107, doi:10.1029/2004GL020560, 2004.

Podolak, M. and Barnum, a.: Moist convection and the abundance of lighning-produced CO, C2H2 and HCN on Jupiter, ICARUS, 75, 566–570, doi:10.1016/0019-1035(88)90165-0, 1988.

Price, C. and Rind, D.: A simple lightning parameterization for calculating global lightning distributions, J. Geophys. Res., 97, 9919–9933, doi:10.1029/92JD00719, 1992.

Randel, W. J., Park, M., Emmons, L., Kinnison, D., Pernath, P., Walker, K. A., Boone, C., and Pumphrey, H.: Asian Monsoon Transport of Pollution to the Stratosphere, Science, 328, 611–613, 2010.

Rinsland, C. P., Goldman, A., Murcray, F. J., Stephen, T. M., Pougatetchev, N. S., Fishman, J., David, S. J., Blatherwick, R. D., Novelli, P. C., Jones, N. B., and Conner, B. J.: Infrared solar spectroscopic measurements of free tropospheric CO, C_2H, and HCN above Mauna Loa, Hawaii: Seasonal variations and evidence for enhanced emissions from the Southeast Asian tropical fires of 1997–1998, J. Geophys. Res., 104, 18667–18680, 1999.

Rinsland, C. P., Mahieu, E., Zander, R., Demoulin, P., Forrer, J., and Buchmann, B.: Free tropospheric CO, C_2H_6, and HCN above central Europe: Recent measurements from the Jungfraujoch station including the detection of elevated columns during 1998, J. Geophys. Res., 105, 24235–24249, 2000.

Rinsland, C. P., Goldman, A., Hannigan, J. W., Wood, S. W., Chiou, L. S., and Mahieu, E.: Long-term trends of tropospheric carbon monoxide and hydrogen cyanide from analysis of high resolution infrared solar spectra, J. Quant. Spectrosc. Radiat. Transfer, 104, 40–51, 2007.

Schneider, J., Burger, V., and Arnold, F.: Methyl cyanide and hydrogen cyanide measurements in the lower stratosphere: Implications for methyl cyanide sources and sinks, J. Geophys. Res., 102, 25501–25506, 1997.

Shim, C., Wang, Y., Singh, H. B., Blake, D. R., and Guenther, A. B.: Source characteristics of oxygenated volatile organic compounds and hydrogen cyanide, J. Geophys. Res., 112, D10305, doi:10.1029/2006JD007543, 2007.

Shindell, D. T., Faluvegi, G., Stevenson, D. S., Krol, M. C., Emmons, L. K., Lamarque, J.-F., Pétron, G., Dentener, F. J., Ellingsen, K., Schultz, M. G., Wild, O., Amann, M., Atherton, C. S., Bergmann, D. J., Bey, I., Butler, T., Cofala, J., Collins, W. J., Derwent, R. G., Doherty, R. M., Drevet, J., Eskes, H. J., Fiore, A. M., Gauss, M., Hauglustaine, D. A., Horowitz, L. W., Isaksen, I. S. A., Lawrence, M. G., Montanaro, V., Müller, J.-F., Pitari, G., Prather, M. J., Pyle, J. A., Rast, S., Rodriguez, J. M., Sanderson, M. G., Savage, N. H., Strahan, S. E., Sudo, K., Szopa, S., Unger, N., van Noije, T. P. C., and Zeng, G.: Multi-model simulations of carbon monoxide: Comparison with observations and projected near-future changes, J. Geophys. Res., 111, D19306, doi:10.1029/2006JD007100, 2006.

Simpson, I. J., Rowland, F. S., Meinardi, S., and Blake, D. R.: Influence of biomass burning during recent fluctuations in the slow growth of global tropospheric methane, Geophys. Res. Lett., 33, L22808, doi:10.1029/2006GL027330, 2006.

Simpson, I. J., Akagi, S. K., Barletta, B., Blake, N. J., Choi, Y., Diskin, G. S., Fried, A., Fuelberg, H. E., Meinardi, S., Rowland, F. S., Vay, S. A., Weinheimer, A. J., Wennberg, P. O., Wiebring, P., Wisthaler, A., Yang, M., Yokelson, R. J., and Blake, D. R.: Boreal forest fire emissions in fresh Canadian smoke plumes: C_1-C_{10} volatile organic compounds (VOCs), CO_2, CO, NO_2, NO, HCN and CH_3CN, Atmos. Chem. Phys., 11, 6445–6463, doi:10.5194/acp-11-6445-2011, 2011.

Singh, H. B., Salas, L., Herlth, D., Kolyer, R., Czech, E., Viezee, W., Li, Q., Jacob, D. J., Blake, D., Sachse, G., Harward, C. N., Fuelberg, H., Kiley, C. M., Zhao, Y., and Kondo, Y.: In situ measurements of HCN and CH_3CN over the Pacific Ocean: sources, sinks, and budgets, J. Geophys. Res., 108, 8795, doi:10.1029/2002JD003006, 2003.

Singh, H. B., Salas, L., Herlth, D., Kolyer, R., Czech, E., Avery, E., Crawford, J. H., Pierce, R. B., Sachse, G., Blake, D. R., Cohen, R. C., Bertram, T. H., Perring, A., Wooldridge, P. J., Dibb, J., Huey, G., Hudman, R. C., Turquety, S., Emmons, L. K., Flocke, F., Tang, Y., Carmichael, G. R., and Horowitz, L. W.: Reactive nitrogen distribution and partitioning in the North American troposphere and lowermost stratosphere, J. Geophys. Res., 112, D12S04, doi:10.1029/2006JD007664, 2007.

Singh, H. B., Cai, C., Kaduwela, A., Weinheimer, A., and Wisthaler, A.: Interactions of fire emissions and urban pollution over California: Ozone formation and air quality simulations, Atmos. Environ., 56, 45–51, 2012.

Sinha, P., Hobbs, P. V., Yokelson, R. J., Bertschi, I. T., Blake, D. R., Simpson, I. J., Gao, S., Kirchstetter, T. W., and Novakov, T.: Emissions of trace gases and particles from savanna fires in Southern Africa, J. Geophys. Res., 108, 8487, doi:10.1029/2002JD002325, 2003.

Slusher, D. L., Huey, L. G., Tanner, D. J., Flocke, F. M., and Roberts, J. M.: A thermal dissociation-chemical ionization mass spectrometry (td-cims) technique for the simultaneous measurement of peroxyacyl nitrates and dinitrogen pentoxide, J. Geophys. Res., 109, D19315, doi:10.1029/2004JD004670, 2004.

Stevenson, D. S., Collins, W. J., Johnson, C. E., and Derwent, R. G.: Intercomparison and evaluation of atmospheric transport in a Lagrangian model (STOCHEM), and an Eulerian model (UM), using Rn-222 as a short-lived tracer, Q. J. Roy. Met. Soc., 124, 2477–2491 doi:10.1256/smsqj.55114, 1998.

Petron, G., Granier, C., Khattatov, B., Yudin, V., Lamarque, J.-F., Emmons, L., Gille, J., and Edwards, D. P.: Monthly CO surface sources inventory based on the 2000-2001 MOPITT satellite data, Geophys. Res. Lett., 31, L21107, doi:10.1029/2004GL020560, 2004.: An inventory of gaseous and primary aerosol emissions in Asia in the year 2000, J. Geophys. Res., 108, 8809, doi:10.1029/2002JD003093, 2003.

Stribling, R. and Miller, S. L.: Electron-discharge synthesis of HCN in simulated jovian atmospheres. ICARUS ICARUS, 72, 48–52, doi:10.1016/0019-1035(87)90117-5, 1987.

Stroppiana, D., Brivio, P. A., Grégoire, J.-M., Liousse, C., Guillaume, B., Granier, C., Mieville, A., Chin, M., and Pétron, G.: Comparison of global inventories of CO emissions from biomass burning derived from remotely sensed data, Atmos. Chem. Phys., 10, 12173–12189, doi:10.5194/acp-10-12173-2010, 2010.

Taylor, J. A., Zimmerman, P. R., and Erickson III, D. J.: A 3-D modelling study of the sources and sinks of atmospheric carbon monoxide, Ecol. Modell., 88, 53–71, 1996.

Tilmes, S., Emmons, L. K., Law, K. S., Ancellet, G., Schlager, H., Paris, J.-D., Fuelberg, H. E., Streets, D. G., Wiedinmyer, C., Diskin, G. S., Kondo, Y., Holloway, J., Schwarz, J. P., Spackman, J. R., Campos, T., Nédélec, P., and Panchenko, M. V.: Source contributions to Northern Hemisphere CO and black carbon during spring and summer 2008 from POLARCAT and START08/preHIPPO observations and MOZART-4, Atmos. Chem. Phys. Discuss., 11, 5935–5983, doi:10.5194/acpd-11-5935-2011, 2011.

Utembe, S. R., Watson, L. A., Shallcross, D. E., and Jenkin, M. E.: A Common Representative Intermediates (CRI) mechanism for VOC degradation. Part 3: Development of a secondary organic aerosol module, Atmos. Environ., 43, 1982–1990, 2009.

Utembe, S. R., Cooke, M. C., Archibald, A. T., Shallcross, D. E., Derwent, R. G., and Jenkin, M. E.: Simulating Secondary Organic Aerosol in a 3-D Lagrangian Chemistry Transport Model using the reduced Common Representative Intermediates Mech-

anism (CRIv2-R5), Atmos. Environ., 45, 1604–1614, 2011.

Val Martin, M., Logan, J. A., Kahn, R. A., Leung, F.-Y., Nelson, D. L., and Diner, D. J.: Smoke injection heights from fires in North America: analysis of 5 years of satellite observations, Atmos. Chem. Phys., 10, 1491–1510, doi:10.5194/acp-10-1491-2010, 2010.

van der Werf, G. R., Randerson, J. T., Giglio, L., Collatz, G. J., Mu, M., Kasibhatla, P. S., Morton, D. C., DeFries, R. S., Jin, Y., and van Leeuwen, T. T.: Global fire emissions and the contribution of deforestation, savanna, forest, agricultural, and peat fires (1997–2009), Atmos. Chem. Phys., 10, 11707–11735, doi:10.5194/acp-10-11707-2010, 2010.

Vay, S. A., Choi, Y., Vadrevu, K. P., Blake, D. R., Tyler, S. C., Wisthaler, A., Hecobian, A., Kondo, Y., Diskin, G. S., Sachse, G. W., Woo, J.-H., Weinheimer, A. J., Burkhart, J. F., Stohl, A., and Wennberg, P. O.: Patterns of CO_2 and radiocarbon across high northern latitudes during International Polar Year 2008, J. Geophys. Res.-Atmos., 116, D14301, doi:10.1029/2011JD015643, 2011.

Vivchar, A. V., Moiseenko, K. B., and Pankratova, N. V.: Estimates of carbon monoxide emissions from wildfires in Northern Eurasia for airquality assessment and climate modeling, Atmos. Ocean. Phys., 46, 281–293, doi:10.1134/S0001433810030023, 2010.

Watson, L. A., Utembe, S. R., Shallcross, D. E., and Jenkin, M. E.: A Common Representative Intermediates (CRI) mechanism for VOC degradation. Part 2: Gas phase mechanism reduction, Atmos. Environ., 42, 7196–7204, 2008.

Wiegele, A., Glatthor, N., Höpfner, M., Grabowski, U., Kellmann, S., Linden, A., Stiller, G., and von Clarmann, T.: Global distributions of C_2H_6, C_2H_2, HCN, and PAN retrieved from MIPAS reduced spectral resolution measurements, Atmos. Meas. Tech., 5, 723–734, doi:10.5194/amt-5-723-2012, 2012.

Yokelson, R. J., Bertschi, I. T., Christian, T. J., Hobbs, P. V., Ward, D. E., and Hao, W. M.: Trace gas measurements in nascent, aged, and cloud-processed smoke from African savanna fires by airborne Fourier Transform Infrared Spectroscopy (AFTIR), J. Geophys. Res., 108, 8478, doi:10.1029/2002JD002322, 2003.

Yokelson, R. J., Karl, T., Artaxo, P., Blake, D. R., Christian, T. J., Griffith, D. W. T., Guenther, A., and Hao, W. M.: The Tropical Forest and Fire Emissions Experiment: overview and airborne fire emission factor measurements, Atmos. Chem. Phys., 7, 5175–5196, doi:10.5194/acp-7-5175-2007, 2007a.

Yokelson, R. J., Urbanski, S. P., Atlas, E. L., Toohey, D. W., Alvarado, E. C., Crounse, J. D., Wennberg, P. O., Fisher, M. E., Wold, C. E., Campos, T. L., Adachi, K., Buseck, P. R., and Hao, W. M.: Emissions from forest fires near Mexico City, Atmos. Chem. Phys., 7, 5569–5584, doi:10.5194/acp-7-5569-2007, 2007b.

Yokelson, R. J., Crounse, J. D., DeCarlo, P. F., Karl, T., Urbanski, S., Atlas, E., Campos, T., Shinozuka, Y., Kapustin, V., Clarke, A. D., Weinheimer, A., Knapp, D. J., Montzka, D. D., Holloway, J., Weibring, P., Flocke, F., Zheng, W., Toohey, D., Wennberg, P. O., Wiedinmyer, C., Mauldin, L., Fried, A., Richter, D., Walega, J., Jimenez, J. L., Adachi, K., Buseck, P. R., Hall, S. R., and Shetter, R.: Emissions from biomass burning in the Yucatan, Atmos. Chem. Phys., 9, 5785–5812, doi:10.5194/acp-9-5785-2009, 2009.

Yurganov, L. N., Duchatelet, P., Dzhola, A. V., Edwards, D. P., Hase, F., Kramer, I., Mahieu, E., Mellqvist, J., Notholt, J., Novelli, P. C., Rockmann, A., Scheel, H. E., Schneider, M., Schulz, A., Strandberg, A., Sussmann, R., Tanimoto, H., Velazco, V., Drummond, J. R., and Gille, J. C.: Increased Northern Hemispheric carbon monoxide burden in the troposphere in 2002 and 2003 detected from the ground and from space, Atmos. Chem. Phys., 5, 563–573, doi:10.5194/acp-5-563-2005, 2005.

Zhao, Y., Strong, K., Kondo, Y., Koike, M., Matsumi, Y., Irie, H., Rinsland, C. P., Jones, N. B., Suzuki, K., Nakajima, H., Nakane, H., and Murata, I.: Spectroscopic measurements of tropospheric CO, C_2H_6, C_2H_2, and HCN in northern Japan, J. Geophys. Res., 107, 4343, doi:10.1029/2001JD000748, 2002.